Separability properties of tripartite states with $U\otimes U\otimes U$ symmetry

T. Eggeling* and R. F. Werner†
Institut für Mathematische Physik, TU Braunschweig, Mendelssohnstrasse 3, 38106 Braunschweig, Germany
(Received 30 October 2000; published 21 March 2001)

We study separability properties in a five-dimensional set of states of quantum systems composed of three subsystems of equal but arbitrary finite Hilbert space dimension. These are the states that can be written as linear combinations of permutation operators, or equivalently, commute with unitaries of the form $U\otimes U\otimes U$. We compute explicitly the following subsets and their extreme points: (1) triseparable states, which are convex combinations of triple tensor products, (2) biseparable states, which are separable for a twofold partition of the system, and (3) states with positive partial transpose with respect to such a partition. Tripartite entanglement is investigated in terms of the relative entropy of tripartite entanglement and of the trace norm.

DOI: 10.1103/PhysRevA.63.042111 PACS number(s): 03.65.Ta, 03.65.Ca, 89.70.+c

I. INTRODUCTION

One of the difficulties in the theory of entanglement is that state spaces are usually fairly high-dimensional convex sets. Therefore, to explore in detail the potential of entangled states, one often has to rely on lower-dimensional ''laboratories.'' An example of this was the role played by a one-dimensional family of bipartite states [1], which has come to be known as ''Werner states.'' In this paper we present a similar laboratory, designed for the study of entanglement between three subsystems. The basic idea is rather similar to [1] and we believe that this set shares many of the virtues with its bipartite counterpart. First, the states have an explicit parametrization as linear combinations of permutation operators. This is helpful for explicit computations. Secondly, there is a ''twirl'' operation that brings an arbitrary tripartite state to this special subset. This proved to be very helpful for the discussion of entanglement distillation of bipartite entanglement: the first useful distillation procedures worked by starting with Werner states, applying a suitable distillation operation, and then the twirl projection to come back to the simple and well-understood subset, thus allowing iteration [2,3]. Geometrically this means that the subset we investigate is both a section of the state space by a plane and the image of the state space under a projection. The basic technique for getting such subsets is averaging over a symmetry group of the entire state space. Such an averaging projection preserves separability if it is an average only over local (factorizing) unitaries. Of course, special subgroups might turn out to be useful. For example, in a recent paper [4] a class of tripartite ($n=3$) states was studied for dimension $d=2$, which is invariant under unitaries of the group of order 24 generated by $\sigma_1^{\otimes 3}$, $\sigma_3\otimes\mathbb{1}\otimes\sigma_3$, $\mathbb{1}\otimes\sigma_3\otimes\sigma_3$, and $\exp(i\pi\sigma_3/3)^{\otimes 3}$.

The third useful property of the states we study is that they can be defined for systems of arbitrary finite Hilbert space dimension d, leading to the same five-dimensional convex set for every d. [This generalizes to an $(n!-1)$-dimensional set for n-partite systems.] Surprisingly, it turns out that the separability sets we investigate are also independent of dimension.

We now describe the natural entanglement (or separability) properties we will chart for these special states. Our classification is similar to the one used in [4], but differs in that we do not artificially make the classes disjoint.

Of course, we can split the system into just two subsystems and apply the usual separability/entanglement distinctions. A split $1|23$ then corresponds to the grouping of the Hilbert space $\mathcal{H}_1\otimes\mathcal{H}_2\otimes\mathcal{H}_3$ into $\mathcal{H}_1\otimes(\mathcal{H}_2\otimes\mathcal{H}_3)$. We call a density operator ρ on this Hilbert space $1|23$-*separable* (or just *biseparable* if the partition is clear from the context) if we can write

$$\rho=\sum_\alpha \lambda_\alpha \rho_\alpha^{(1)}\otimes\rho_\alpha^{(23)}, \tag{1}$$

with $\lambda_\alpha\geqslant 0$ and density operators $\rho_\alpha^{(23)}$ on $\mathcal{H}_2\otimes\mathcal{H}_3$. We will denote the set of such ρ by $\mathcal{B}_1$. This set will be computed in Sec. V. Furthermore, as it is a necessary condition for biseparability (cf. Peres [5]), we are going to look at those states ρ having a *positive partial transpose* with regard to such a split denoted by $\rho\in\mathcal{P}_1$. Recall that the partial transpose $A\mapsto A^{T_1}$ of operators on $\mathcal{H}_1\otimes\mathcal{H}_2$ is defined by

$$\left(\sum_\alpha A_\alpha\otimes B_\alpha\right)^{T_1}=\sum_\alpha A_\alpha^T\otimes B_\alpha, \tag{2}$$

where A^T on the right-hand side is the ordinary transposition of matrices with respect to a fixed basis. It is clear that $\mathcal{B}_1\subset\mathcal{P}_1$ holds, but as we will show in Sec. VI by computing $\mathcal{P}_1$, this inclusion is strict except for $d=2$.

As a genuinely ''tripartite'' notion of separability, we consider states, called *triseparable* (or ''three-way classically correlated''), which can be decomposed as

$$\rho=\sum_\alpha \lambda_\alpha \rho_\alpha^{(1)}\otimes\rho_\alpha^{(2)}\otimes\rho_\alpha^{(3)}, \tag{3}$$

where $\lambda_\alpha\geqslant 0$ and the $\rho_\alpha^{(i)}$ are density operators on the respective Hilbert spaces. The set of such density operators will be denoted by $\mathcal{T}$. Of course, we may also consider states that are biseparable for all three partitions. It is known [6] that this

*Electronic address: T.Eggeling@tu-bs.de
†Electronic address: R.Werner@tu-bs.de

does not imply triseparability, i.e., $\mathcal{T}\subsetneqq(\mathcal{B}_1\cap\mathcal{B}_2\cap\mathcal{B}_3)$. Further examples will be found below.

Since in this paper we will only be interested in a five-dimensional set $\mathcal{W}$ of symmetric states (see the next section), we will from now on use the symbols $\mathcal{T}$, $\mathcal{B}_1$, and $\mathcal{P}_1$ only for the corresponding subsets of $\mathcal{W}$.

II. DEFINITION AND MAIN RESULTS

A. $U\otimes U\otimes U$-invariant states: $\mathcal{W}$

Throughout we consider states on a Hilbert space of the form $\mathcal{H}\otimes\mathcal{H}\otimes\mathcal{H}$, where $\mathcal{H}$ is a Hilbert space of finite dimension d. The group of permutations on three elements acts on this space by unitary operators V_π, defined by

$$V_\pi\,\phi_1\otimes\phi_2\otimes\phi_3=\phi_{\pi^{-1}1}\otimes\phi_{\pi^{-1}2}\otimes\phi_{\pi^{-1}3}.$$

For the six permutations π we use cycle notation so that $V_{(12)}$ is the permutation operator of the first two factors and $V_{(123)}$ is the cyclic permutation taking 1 to 2. We denote by "dU" the normalized Haar measure on the unitary group of $\mathcal{H}$ and define on the space of operators the operator

$$\mathbf{P}\rho=\int dU(U\otimes U\otimes U)\rho(U\otimes U\otimes U)^*. \qquad (4)$$

Clearly, $\mathbf{P}$ takes positive operators to positive operators (it is even completely positive) and $\mathrm{tr}(\mathbf{P}\rho)=\mathrm{tr}(\rho)$, i.e., $\mathbf{P}$ maps density operators to density operators. We can now define the set of states, which form the object of our investigation.

Lemma 1. For an operator ρ on $\mathcal{H}\otimes\mathcal{H}\otimes\mathcal{H}$ the following conditions are equivalent:

(1) $(U\otimes U\otimes U)\rho=\rho(U\otimes U\otimes U)$ for all unitary operators U on $\mathcal{H}$.

(2) $\mathbf{P}\rho=\rho$.

(3) $\rho=\Sigma_\pi\mu_\pi V_\pi$ with coefficients $\mu_\pi\in\mathbb{C}$.

The set of density operators satisfying these conditions will be denoted by $\mathcal{W}$.

The equivalence of Eqs. (1) and (2) is straightforward from the invariance of the Haar measure. The implication $(3)\Rightarrow(1)$ is trivial because the permutation operators clearly commute with operators of the form $(U\otimes U\otimes U)$. The only nontrivial part is thus $(1)\Rightarrow(3)$, which is, however, a standard result ([7], Chap. IV) from representation theory. Of course, all these work for any number of tensor factors.

The above Lemma does not address the question how to recognize density matrices in terms of the six coefficients μ_π. Hermiticity requires $\mu_{\pi^{-1}}=\overline{\mu_\pi}$, leaving effectively six real parameters. One more is fixed by normalization so that $\mathcal{W}$ is embedded in a five-dimensional real vector space. In terms of the parameters μ_π positivity is not easy to see. In order to get a better criterion, it is best to study the *algebra* of operators that are linear combinations of the permutations. The product of such operators can readily be computed by using only the multiplication law for permutations. The abstract algebra of formal linear combinations of group elements (known as the group algebra) can be decomposed in terms of the irreducible representations of the underlying group, suggesting a basis that is much more handy for deciding positivity. Again, this step works for any number of factors, but we carry it out only in the case $n=3$. We introduce the following linear combinations of permutation operators:

$$R_+=\frac{1}{6}(\mathbb{1}+V_{(12)}+V_{(23)}+V_{(31)}+V_{(123)}+V_{(321)}), \qquad (5a)$$

$$R_-=\frac{1}{6}(\mathbb{1}-V_{(12)}-V_{(23)}-V_{(31)}+V_{(123)}+V_{(321)}), \qquad (5b)$$

$$R_0=\frac{1}{3}(2\cdot\mathbb{1}-V_{(123)}-V_{(321)}), \qquad (5c)$$

$$R_1=\frac{1}{3}(2V_{(23)}-V_{(31)}-V_{(12)}), \qquad (5d)$$

$$R_2=\frac{1}{\sqrt{3}}(V_{(12)}-V_{(31)}), \qquad (5e)$$

$$R_3=\frac{i}{\sqrt{3}}(V_{(123)}-V_{(321)}). \qquad (5f)$$

Then R_+, R_-, and R_0 are orthogonal projections adding up to $\mathbb{1}$ and commute with all permutations. This means that they correspond to the irreducible representations of the permutation group: R_+ and R_- correspond to the two one-dimensional representations (trivial and alternating representation, respectively), and these operators are indeed just the orthogonal projections onto the symmetric and antisymmetric subspaces of $\mathcal{H}\otimes\mathcal{H}\otimes\mathcal{H}$ in the usual sense. Their complement R_0 corresponds to a two-dimensional representation, which is hence isomorphic to the 2×2-matrices. The operators R_1, R_2, and R_3 act as the Pauli matrices of this representation. In other words, the six hermitian operators R_+, R_-, R_0, R_1, R_2, and R_3 are characterized by the commutation relations $R_iR_\pm=R_\pm R_i=0$, $R_i^2=R_0$, for $i=0$, 1, 2, and 3 and $R_1R_2=iR_3$ with cyclic permutations.

Now every operator ρ in the linear span of the permutations can be decomposed into the orthogonal parts $R_+\rho$, $R_-\rho$, and $R_0\rho$ and positivity of ρ is equivalent to the positivity of all three operators. This leads to the following Lemma:

Lemma 2. For any operator ρ on $\mathcal{H}\otimes\mathcal{H}\otimes\mathcal{H}$, define the six parameters $r_k(\rho)=\mathrm{tr}(\rho R_k)$, for $k\in\{+,-,0,1,2,3\}$. Then $r_k(\mathbf{P}\rho)=r_k(\rho)$. Moreover, each $\rho\in\mathcal{W}$ is uniquely characterized by the tuple $(r_+,r_-,r_0,r_1,r_2,r_3)\in\mathbb{R}^6$ and such a tuple belongs to a density matrix $\rho\in\mathcal{W}$ if and only if

$$r_+,r_-,r_0\geq0,\quad r_++r_-+r_0=1,$$

$$r_1^2+r_2^2+r_3^2\leq r_0^2. \qquad (6)$$

Note that in this parametrization the set $\mathcal{W}$ does not depend on the dimension d with one exception: for $d=2$ the antisymmetric projection R_- is simply zero, so for qubits we get the additional constraint $r_-=0$. If one considers a given

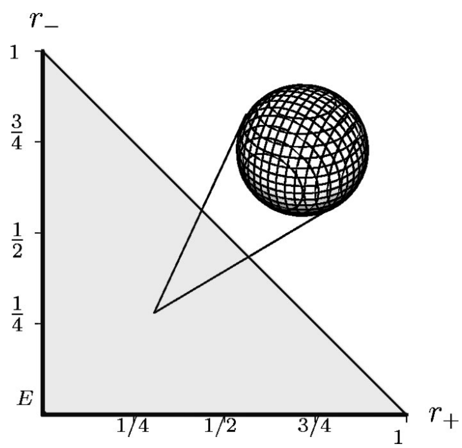

FIG. 1. Description of $\mathcal{W}$ in terms of the triangle $\mathcal{W}^P$ and the corresponding Bloch sphere for each point in $\mathcal{W}^P$.

density operator ρ as an operator ρ' in $\mathcal{H}'\otimes\mathcal{H}'\otimes\mathcal{H}'$ for a higher-dimensional space $\mathcal{H}'\supset\mathcal{H}$, by setting all ''new'' matrix elements equal to zero, we will have $r_k(\rho)=r_k(\rho')$.

Taking $r_0=1-r_+-r_-$ to be redundant, we get a simple representation of $\mathcal{W}$ as a convex set in five dimensions. Unfortunately, five-dimensional sets are still not very amenable to graphical representation. For visualizing the sets we are going to describe analytically, we will therefore use suitable two- and three-dimensional representations. Again, we have the possibility of using sections or projections of $\mathcal{W}$ and we will emphasize sections that can also be understood as projections.

The simplest example of this is to take the subset $\mathcal{W}^P\subset\mathcal{W}$ of states, which also commute with all permutations. The corresponding projection is simply averaging with respect to permutations. Clearly, $\mathcal{W}^P$ consists of those operators in $\mathcal{W}$, which are linear combinations of R_+, R_-, and R_0 alone. Taking r_+ and r_- as coordinates, we get the triangle in Fig. 1. Thus each point in this triangle represents a density operator in $\mathcal{W}^P$. On the other hand, it represents the set of states in $\mathcal{W}$ projecting to it on permutation averaging: this will be all states with the given values of r_+ and r_- in the 6-tuple, which therefore differ only in the values of r_1, r_2, and r_3. Thus, over every point of the triangle in Fig. 1, we should imagine a Bloch sphere of radius r_0.

If more detail is required, we will also use three-dimensional sections and/or projections of a similar nature. For example, if we average only over the permutations $V_{(23)}$, we get the subset $\mathcal{W}^{(23)}\subset\mathcal{W}$ with $r_2=r_3=0$ (see the dotted tetrahedron in Fig. 10). Averaging only over cyclic permutations, we get the subset $\mathcal{W}^{\mathrm{cyc}}\subset\mathcal{W}$ with $r_1=r_2=0$ (which gives the same tetrahedron as $\mathcal{W}^{(23)}$ with r_1 substituted by r_3).

We note for later use that the expectation values r_k are *not* the coefficients in the sum

$$\rho=\sum_{k=+,-,0,1,2,3} c_k R_k. \tag{7}$$

These are related to the parameters r_k by the following dimension-dependent transformation [which is obtained by observing that $\mathrm{tr}\,\mathbb{1}=d^3$, $\mathrm{tr}(V_{(12)})=d^2$, and $\mathrm{tr}(V_{(123)})=d$]:

$$r_+=\frac{d}{6}(d^2+3d+2)c_+, \tag{8a}$$

$$r_-=\frac{d}{6}(d^2-3d+2)c_-, \tag{8b}$$

$$r_i=\frac{2d}{3}(d^2-1)c_i \quad \text{for } i=0,1,2,3. \tag{8c}$$

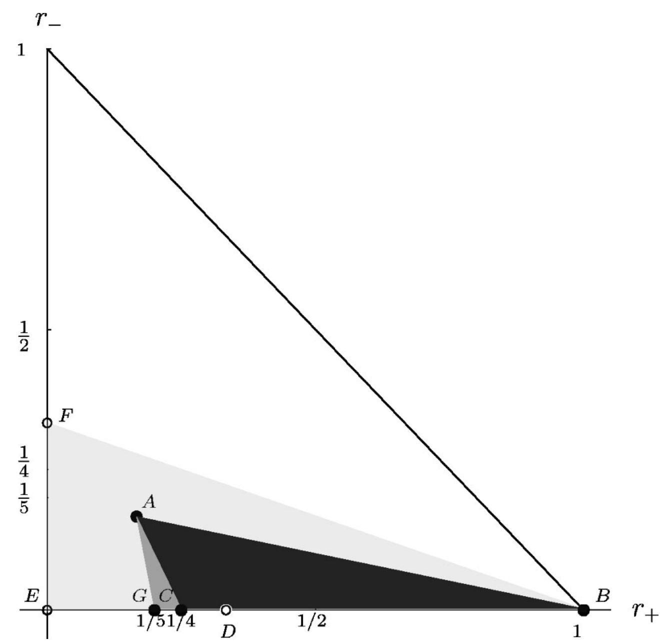

FIG. 2. Subsets of $\mathcal{W}^P$ with different separability properties. Black triseparable; dark gray, biseparable; and light gray, images of biseparable states under permutation averaging. Special points explained in the text.

B. Overview of main results

An overview of the main results of this paper is given in Fig. 2. To keep the picture as simple as possible, we have only depicted the set $\mathcal{W}^P$, i.e., the triangle in Fig. 1. Naturally, this reduction does not allow the representation of our full results, i.e., the detailed structure of the five-dimensional convex sets $\mathcal{T}$, $\mathcal{B}_1$, and $\mathcal{P}_1$, which will be described in the corresponding sections. However, we found this diagram quite useful as a basic map for not losing our way in five dimensions, and hope it will similarly serve our readers.

The shading in Fig. 2 marks different separability properties and the points labeled with capital letters arise by projecting pure states with special properties with the twirl projection (4). Some of these points (D,E,F) do not lie in the plane $\mathcal{W}^P$, i.e., they have nonzero coordinates (r_1,r_2,r_3). They are represented by white circles, in contrast to the black circles (A,B,C,G,H) representing permutation invariant states in the plane $\mathcal{W}^P$.

The *triseparable* states correspond to the black triangle $\triangle(ABC)$. It is easy to see that any triseparable state projected by permutation averaging to $\mathcal{W}^P$ is again triseparable, i.e., the projection of $\mathcal{T}$ onto $\mathcal{W}^P$ coincides with $\mathcal{T}\cap\mathcal{W}^P$. The extreme points of this set are

$$A:|123\rangle\rightarrow(1/6,1/6,0,0,0),$$

$$B:|111\rangle\rightarrow(1,0,0,0,0),$$

$$C:(|111\rangle-\sqrt{3}|112\rangle+\sqrt{3}|121\rangle-3|122\rangle)/4\rightarrow(1/4,0,0,0,0),$$

where the notation $\Psi\rightarrow(r_+,r_-,r_1,r_2,r_3)$ indicates that the pure state $|\Psi\rangle\langle\Psi|$ is projected to this point by $\mathbf{P}$ from Eq. (4). In other words, $\langle\Psi|R_k\Psi\rangle=r_k$ for $k=+,-,1,2,3$. Note that all three vectors given are product vectors, the one for C being the product of three vectors in the ''Mercedes star'' configuration in the plane, at an angle 120° from each other.

A quantitative description of the genuinely tripartite entanglement of $\mathcal{W}$ is given in Sec. IV in terms of the relative entropy and the trace norm.

The *biseparable* set $\mathcal{B}_1$ is not permutation invariant since the partition $1|23$ clearly is not. As a consequence, the permutation average projecting $\mathcal{W}$ onto $\mathcal{W}^P$ does not map $\mathcal{B}_1$ into itself, and we have to distinguish in our diagram between points (r_+,r_-) such that $(r_+,r_-,0,0,0)$ is biseparable (i.e., the *intersection* $\mathcal{B}_1\cap\mathcal{W}^P$) and points (r_+,r_-) such that for some suitable (r_1,r_2,r_3), the quintuple (r_+,r_-,r_1,r_2,r_3) represents a point in $\mathcal{B}_1$, (i.e., the *projection* of $\mathcal{B}_1$ onto $\mathcal{W}^P$). In Fig. 2 the intersection is the triangle $\triangle(GAB)$, drawn in a darker shade of gray than the triangle $\triangle(EFB)$, which is the projection of the biseparable subset $\mathcal{B}_1$. Note that the shading reflects the inclusion relations, i.e., triseparable states are, in particular, biseparable, and the section of the biseparable set is contained in its projection. Of course, the states in $\mathcal{B}_1\cap\mathcal{W}^P$ are also biseparable for the other two partitions since they are permutation invariant. Similarly, the projections of $\mathcal{B}_2$ and $\mathcal{B}_3$ onto $\mathcal{W}^P$ are the same.

Points of special interest for the biseparable set arise from the following vectors:

$$D:|122\rangle\rightarrow(1/3,0,2/3,0,0),$$

$$E:(|112\rangle-|121\rangle)/\sqrt{2}\rightarrow(0,0,-1,0,0),$$

$$F:(|123\rangle-|132\rangle)/\sqrt{2}\rightarrow(0,1/3,-2/3,0,0),$$

$$G:(|112\rangle-|121\rangle-\sqrt{3}|122\rangle)/\sqrt{5}\rightarrow(1/5,0,0,0,0).$$

Here the points B, D, E, and F are extreme points of $\mathcal{B}_1$ and span a tetrahedron, which is equal to the subset $\mathcal{B}_1\cap\mathcal{W}^{(23)}$ of states invariant under the exchange $2\leftrightarrow3$. The point G lies on the line connecting E and D and is the unique extreme point of $\mathcal{B}_1\cap\mathcal{W}^P$ which is not triseparable. In this sense it represents an extreme case demonstrating the inequality $\mathcal{T}\neq(\mathcal{B}_1\cap\mathcal{B}_2\cap\mathcal{B}_3)$.

The set $\mathcal{P}_1$ of states with *positive partial transpose* with respect to the partition $1|23$ contains $\mathcal{B}_1$ strictly but the difference cannot be seen in this diagram. In fact, we will show in Sec. VI that even the 23-invariant subsets of $\mathcal{P}_1$ and $\mathcal{B}_1$ coincide, i.e., $\mathcal{P}_1\cap\mathcal{W}^{(23)}$ is spanned by the same four extreme points B, D, E, and F.

As will be seen in Sec. VI, there is a close connection between the problems of finding $\mathcal{P}_1$ and finding states invariant under averaging over all unitaries of the form $\bar{U}\otimes U\otimes U$. It turns out that the sets of triseparable and biseparable states commuting with such unitaries can be obtained via a simple linear transformation from their counterparts $\mathcal{T}\cap\mathcal{W}$ and $\mathcal{B}_1\cap\mathcal{W}$ computed in this paper. This mapping and a sketch of the results is given in the Appendix.

III. TRISEPARABLE STATES: $\mathcal{T}$

If ρ is triseparable and hence has a decomposition of the form (3), we may also find a decomposition in which all factors $\rho_\alpha^{(i)}$ are pure, simply by decomposing each of these density operators into pure ones. Applying to such a decomposition the projection $\mathbf{P}$, we find that $\rho\in\mathcal{T}\subset\mathcal{W}$ if and only if ρ is a convex combination of states of the form $\mathbf{P}(|\Psi\rangle\times\langle\Psi|)$, where $\Psi=\psi_1\otimes\psi_2\otimes\psi_3$ is a normalized product vector. Let us denote by $\mathcal{T}_{\rm pure}\subset\mathcal{W}$ the set of such states. Our strategy for determining $\mathcal{T}$ will be to first get $\mathcal{T}_{\rm pure}$ and then to obtain $\mathcal{T}$ as its convex hull. The resulting characterization of $\mathcal{T}$ is formulated in Theorem 1.

Given a product vector $\Psi=\psi_1\otimes\psi_2\otimes\psi_3$, it is easy to compute the projected state $\mathbf{P}(|\Psi\rangle\langle\Psi|)$: By Lemma 2 one just has to compute the expectations of the permutation operators. For example,

$$\langle\Psi|V_{(12)}\Psi\rangle=\langle\psi_1\otimes\psi_2\otimes\psi_3|\psi_2\otimes\psi_1\otimes\psi_3\rangle=|\langle\psi_1|\psi_2\rangle|^2.$$

In this way it is easily seen that the expectations of all permutations are $\{1,a_1,a_2,a_3,a_4+ia_5,a_4-ia_5\}$, where the five real parameters are given by

$$a_1=|\langle\psi_2|\psi_3\rangle|^2, \tag{9a}$$

$$a_2=|\langle\psi_3|\psi_1\rangle|^2, \tag{9b}$$

$$a_3=|\langle\psi_1|\psi_2\rangle|^2, \tag{9c}$$

$$a_4=\mathrm{Re}(\langle\psi_1|\psi_2\rangle\langle\psi_2|\psi_3\rangle\langle\psi_3|\psi_1\rangle), \tag{9d}$$

$$a_5=\mathrm{Im}(\langle\psi_1|\psi_2\rangle\langle\psi_2|\psi_3\rangle\langle\psi_3|\psi_1\rangle). \tag{9e}$$

Since a pure state in d dimensions (taken up to a factor) is given by $2d-2$ real parameters, these five quantities are a considerable reduction from the $6(d-1)$ parameters determining the three vectors ψ_i. However, they are still not independent due to the identity

$$f(a_1,a_2,a_3,a_4,a_5):=a_4^2+a_5^2-a_1a_2a_3=0. \tag{10}$$

Since we want to determine $\mathcal{T}_{\rm pure}$ exactly, we also have to find the exact range of these parameters, as the ψ_i vary over all unit vectors. This is done in the following lemma.

Lemma 3. A tuple $(a_1,a_2,a_3,a_4,a_5)\in\mathbb{R}^5$ *arises via* Eq. (9) *from three unit vectors* ψ_1,ψ_2,ψ_3 *in a d-dimensional Hilbert space* $(d>3)$ *if and only if* Eq. (10) *is satisfied*, $0\leqslant a_i\leqslant 1$ *for* $i=1,2,3$, *and*

$$1-a_1-a_2-a_3+2a_4\geqslant 0. \tag{11}$$

If $d=2$ *the Lemma holds with last inequality replaced by equality*.

Proof. Necessity of Eq. (10) and $0\leqslant a_i\leqslant 1$ is clear. Inequality (11) is just the condition that the expectation of antisymmetric projection should be positive. Since this projection vanishes for $d=2$, it is also clear that equality must hold in this case.

Suppose now that $a_1,\ldots,a_5$ satisfying these constraints are given. We have to reconstruct ψ_1, ψ_2, and ψ_3 satisfying Eq. (9). These equations essentially determine the 3×3-matrix $M_{ij}=\langle\psi_i|\psi_j\rangle$ of scalar products. Of course, we already know the absolute values of its entries (note $M_{ii}=1$). The phases are irrelevant up to some extent: multiplying any row with a phase and the corresponding column with its complex conjugate will not change a_i after Eq. (9) and amounts to multiplying one of the ψ_i with a phase. Hence we may assume that the scalar products $\langle\psi_1|\psi_2\rangle$ and $\langle\psi_2|\psi_3\rangle$ are positive. The phase of the remaining scalar product $\langle\psi_3|\psi_1\rangle$ is then the same as the phase of a_4+ia_5, hence M is essentially uniquely determined by the parameters a_i.

Now M is a matrix of scalar products if and only if it is positive definite: on one hand, $\Sigma_{ij}\overline{u_i}u_jM_{ij}=\|\Sigma_iu_i\psi_i\|^2\geqslant 0$ and on the other, we can construct a Hilbert space with such scalar products as the space of formal linear combinations of three vectors with scalar products of basis vectors *defined* by M. Positive definiteness of M then ensures the positivity of the norm in this new Hilbert space. The dimension of this space is the rank of M (number of linearly independent rows/columns). So in the present case the dimension will be 3 (but any larger space will also contain appropriate vectors) or $\leqslant 2$ if M is a singular matrix.

Positive definiteness of M is equivalent to the positivity of all subdeterminants. The diagonal elements are 1, hence positive anyway. Positivity of the three 2×2-subdeterminants is equivalent to $a_i\leqslant 1$ for $i=1,2,3$. Finally, the full determinant of M, expressed in terms of a_i gives expression (11). It must be positive, and for $d=2$ it must vanish since M is singular. ■

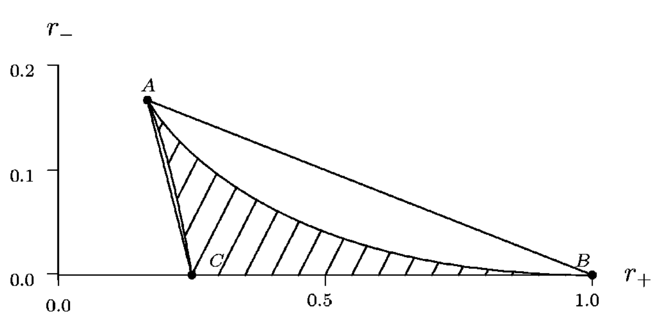

FIG. 3. Section of the set $\mathcal{T}_{\rm pure}$ with $\mathcal{W}^P$ and its convex hull.

Lemma 3 describes the set $\mathcal{T}_{\rm pure}$ of projected pure product states as a compact subset of the hypersurface in $\mathbb{R}^5$ defined by Eq. (10). Computing the convex hull of this set in $\mathbb{R}^5$ is the same as computing the convex hull of $\mathcal{T}_{\rm pure}$ because the expectations of permutations or the operators R_k from Eq. (5) are affine functions of a_i. Explicitly, the expectations $r_k=\langle\Psi|R_k\Psi\rangle$, $k=+,-,0,1,2,3$, which we have used as our standard coordinates in $\mathcal{W}$ are

$$r_+=\frac{1}{6}\{1+(a_1+a_2+a_3)+2a_4\},$$

$$r_-=\frac{1}{6}\{1-(a_1+a_2+a_3)+2a_4\},$$

$$r_0=\frac{2}{3}(1-a_4),$$

$$r_1=\frac{1}{3}(2a_1-a_2-a_3),$$

$$r_2=\frac{1}{\sqrt{3}}(a_3-a_2),$$

$$r_3=\frac{2}{\sqrt{3}}a_5.$$

We begin by computing the projection of $\mathcal{T}_{\rm pure}$ onto the (r_+,r_-) plane by determining the possible range of the combinations $m=(a_1+a_2+a_3)/3$ and a_4. By choosing phases for the scalar products we can make a_4 vary in the range $|a_4|\leqslant(a_1a_2a_3)^{1/2}=g^{3/2}$, where m and g are the arithmetic and the geometric means of a_1, a_2, and a_3. As is well known, $g\leqslant m$ and equality holds if $a_1=a_2=a_3$. Hence the projection of $\mathcal{T}_{\rm pure}$ is contained between the parametrized lines

$$r_+(m)=\frac{1}{6}(1+3m\pm 2m^{2/3}),$$

$$r_-(m)=\frac{1}{6}(1-3m\pm 2m^{2/3}).$$

Plotting these curves gives Fig. 3. It is clear that the shape is not convex and its convex hull is the triangle ABC.

A similar plot of the set $\mathcal{T}_{\rm pure}$ including one more coordinate, r_3, is given in Fig. 4.

Again, it is clear that no point on the surface can be an extreme point of the convex hull of the surface because the surface ''curves the wrong way.'' This is the intuition behind the following lemma by which we will show that also in the full five-dimensional case, the interior of $\mathcal{T}_{\rm pure}$ contains no extreme points.

Lemma 4. Let $N_f=\{x\in\mathbb{R}^n|f(x)=0\}$ *be the zero surface of a function* $f\in\mathcal{C}^2(\mathbb{R}^n,\mathbb{R})$ *and* $K\subset\mathbb{R}^n$ *a compact convex set. Let* $\mathcal{U}$ *be an open ball around a point* $x_h\in N_f$ *such that* $(\mathcal{U}\cap N_f)\subset K$, *and suppose that* x_h *is hyperbolic in the fol-*

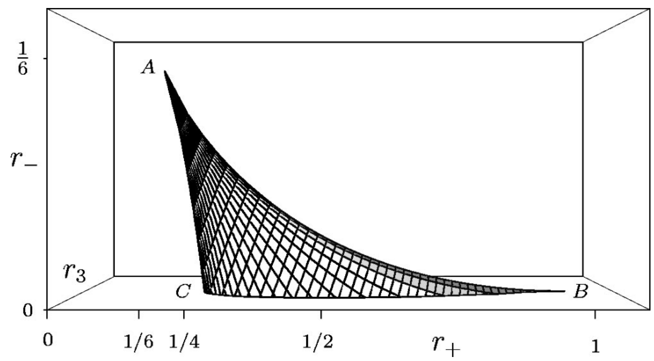

FIG. 4. Plot of the same section as above making additional use of the coordinate r_3.

lowing sense: $\nabla f(x_h)\neq 0$ *and the tangent plane through* x_h *contains two lines such that the second derivative of f is strictly positive along one and strictly negative along the other. Then* x_h *is not an extreme point of K.*

Proof. Suppose x_h is an extreme point of K. Then there must be a supporting hyperplane, i.e., a hyperplane H through x_h such that K lies entirely in one of the closed subspaces bounded by H. We claim that this implies that f, restricted to H, has to be either non-negative or nonpositive in a neighborhood of x_h.

Suppose on the contrary there are points $x_+,x_-\in H\cap\mathcal{U}$ such that $f(x_+)>0>f(x_-)$. We may then connect x_+ and x_- by a continuous curve lying entirely in $\mathcal{U}$ and also in one of the two open half spaces bounded by H. Since f is continuous, any such curve must contain a point y with $f(y)=0$, i.e., $y\in(N_f\cap\mathcal{U})\subset K$. Since we can choose either side of H for the connection, we find points $y\in K$ on both sides of H, hence H cannot be a supporting hyperplane.

This argument shows, in the first instance, that the only possible supporting hyperplane at x_h is the tangent hyperplane (look at the Taylor approximation of f to first order). Applying the argument with the second-order Taylor approximation, we find that hyperbolic points cannot have supporting hyperplanes, hence cannot be extremal. ■

To apply this lemma to the function f from Eq. (10), we have to pick two appropriate tangent lines at any given point $\vec{a}=(a_1,a_2,a_3,a_4,a_5)$ on the surface. We parameterize such lines as $\vec{a}+t\vec{b}$, $t\in\mathbb{R}$ so that $f(\vec{a}+t\vec{b})=f(\vec{a})+Mt^2$. Two choices with an opposite sign of M are

$$\vec{b}=(0,0,0,a_5,-a_4),\quad M=(a_4^2+a_5^2),$$

$$\vec{b}=(2a_1,2a_2,2a_3,3a_4,3a_5),\quad M=-3(a_4^2+a_5^2),$$

where we have used the equation $f(\vec{a})=0$ to evaluate the last expression. Hence every point of the surface N_f is hyperbolic.

By Lemma 4 we therefore only have to consider boundary points of the surface, i.e., points for which at least one of the inequalities in Lemma 3 is an equality.

Let us begin with the equalities $a_i=0$, for at least one $i\in\{1,2,3\}$. Then we have $a_4=a_5=0$ by Eq. (10) and $0\leqslant a_j+a_k\leqslant 1$ $(j\neq k)$ by Eq. (11). As we are looking for extremal points, we are left with the cases $a_j=a_k=0$ representing the triorthogonal states [8] [i.e., point $A=(\frac{1}{6},\frac{1}{6},0,0,0)$ in r_i's] or $a_j+a_k=1$. All such points satisfy $r_-=0$, hence they will be in our general discussion of cases with $r_-=0$. The equalities $a_i=1$ lead via Eq. (11) to the inequality $0\leqslant 2a_4-(a_j+a_k)$ and therefore, to

$$a_4\geqslant\tfrac{1}{2}(a_j+a_k)\geqslant\sqrt{a_ja_k}=\sqrt{a_ia_ja_k}$$
$$=\sqrt{a_4^2+a_5^2}\geqslant\sqrt{a_4^2}=|a_4|\geqslant a_4.$$

From this we can see that $a_5=0$, $a_j=a_k$, and $a_4=a_j=a_k$. Once again this implies $r_-=0$ so that this remains the only case to be checked.

For $r_-=0$, we can express a_i by r_+, r_1, r_2, and r_3, and solve Eq. (10) for r_3, obtaining a relation of the form

$$r_3=\pm h(r_+,r_1,r_2),\tag{12}$$

where h is the square root of a third-order polynomial. Equation (12) describes the surface of a convex set if h is a concave function. This can be checked by verifying that the Hessian of h is everywhere negative semidefinite. Hence all points in $\mathcal{T}_{\rm pure}$ with $r_-=0$ are extremal and are characterized by Eq. (12). This completes the determination of extreme points of $\mathcal{T}$, summarized in the following Theorem. It also contains the dual description of $\mathcal{T}$ in terms of inequalities.

Theorem 1. The subset $\mathcal{T}\subset\mathcal{W}$ *of triseparable states has the following extreme points, described here in terms of the expectations* $r_k={\rm tr}(\rho R_k)$, $k=+,-,1,2,3$.

(1) $3r_3^2+(1-3r_+)^2=(r_1+r_+)(r_1-\sqrt{3}r_2-2r_+)(r_1+\sqrt{3}r_2-2r_+)$ and $r_-=0$,

(2) *The point* $A=(1/6,1/6,0,0,0)$.

A state $\rho\in\mathcal{W}$ *is triseparable if and only if it corresponds to the point A or the following inequalities are satisfied*:

(a) $0\leqslant r_-<\frac{1}{6}$.

(b) $\frac{1}{4}(1-2r_-)\leqslant r_+\leqslant 1-5r_-$,

(c) $(3r_3^2+[1-3r_+-3r_-]^2)(1-6r_-)\leqslant(r_1+r_+-r_-)\times\{(r_1-2[r_+-r_-])^2-3r_2^2\}$.

These inequalities are obtained by projecting the given point onto the hyperplane $r_-=0$ from point A and checking whether the projected point satisfies the inequality $|r_3|\leqslant h(r_+,r_1,r_2)$ with h from Eq. (12). To get an idea of the shape of $\mathcal{T}$ we compute the section with $r_+=0.27$ and $r_-=0.1$ (Fig. 5).

IV. RELATIVE ENTROPY OF TRIPARTITE ENTANGLEMENT

Quantitative measures of bipartite entanglement and their properties are a very active area of research at the moment. In the tripartite case, the difficulties in quantifying entanglement began already with the pure states, for which no canonical form as simple as the Schmidt decomposition exists. One can, however, extend the standard definition of the relation ''more entangled than'' to tripartite states. It is clear as to what local quantum operations should be in the multipartite case, and we can describe classical communication be-

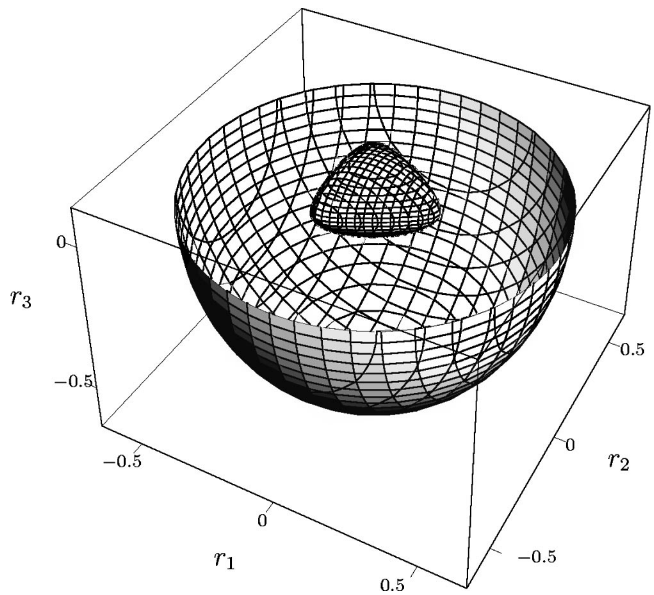

FIG. 5. Plotting the set $\mathcal{T}$ for the section $r_+ = 0.27$ and $r_- = 0.1$ gives a heart-shaped surface with trigonal symmetry which is contained in the respective Bloch sphere.

tween many partners in much the same way as in the bipartite case. Once we fix the rules of classical communication (e.g., ''each partner may broadcast her results to all the others''), we will say that ρ is more entangled than σ, whenever we can reach σ from ρ by a sequence of local operations and classical communication (LOCC), in which case we will write $\rho \succ \sigma$.

A full characterization of this partial-order relation is only known in the case of bipartite pure states (Nielsen's theorem [9]). Even in the mixed bipartite case there is no straightforward way of deciding whether one of two given density operators is more entangled than the other. Hence we cannot hope to give such a characterization in the tripartite case. Nevertheless, the entanglement ordering is one of the features one would like to explore and chart in $\mathcal{W}$. There are two ways of approaching this: on the one hand, we may start from some state $\rho \in \mathcal{W}$, apply many LOCC operations to it, and see where we end up. We can always assume the operation to end up in $\mathcal{W}$, because the twirl operation is itself a LOCC operation, which involves the random choice of U by any one of the partners, the broadcasting of U to the other two partners, and the unitary transformation by U at each of the sites. For an initial survey, we may even study the relation in the permutation invariant triangle $\mathcal{W}^P$ even though the permutation of sites is definitely *not* a local operation. But if the initial state is permutation invariant and T is any LOCC operation involving certain specified tasks for Alice, Bob, and Charly, the three may just throw dice to decide who is to take which role. With this procedure they effectively get the permutation average of the output state of T. With such studies, we get sufficient conditions for $\rho \succ \sigma$.

In order to get necessary conditions the only approach is to find functionals on the state space that are monotone with respect to entanglement ordering. Luckily, one of the ideas for getting such monotones can be transferred from the bipartite case. Obviously, the triseparable subset is invariant under LOCC operations, so the distance to $\mathcal{T}$ is an entanglement monotone provided the distance functional has appropriate properties. One needs only one condition for a function Δ to define an appropriate ''distance'' $\Delta(\rho,\sigma)$ between arbitrary states of the same tripartite system.

$$\Delta(T\rho,T\sigma) \leqslant \Delta(\rho,\sigma) \quad \text{for any LOCC operation } T. \tag{13}$$

Then for the functional

$$E_\Delta(\rho) = \inf\{\Delta(\rho,\sigma) | \sigma \in \mathcal{T}\} \tag{14}$$

we get the inequalities

$$E_\Delta(T\rho) \leqslant \inf\{\Delta(T\rho,\sigma) | \sigma = T\sigma'; \quad \sigma' \in \mathcal{T}\} \tag{15}$$

$$= \inf\{\Delta(T\rho,T\sigma') | \sigma' \in \mathcal{T}\} \tag{16}$$

$$\leqslant \inf\{\Delta(\rho,\sigma') | \sigma' \in \mathcal{T}\} = E_\Delta(\rho). \tag{17}$$

Hence E_Δ is indeed a decreasing functional with respect to the ordering $\succ$. Note that the only property of $\mathcal{T}$ needed to show this is that it is mapped into itself under LOCC operations. Any other set with this property (e.g., $\mathcal{B}_1$ or $\mathcal{P}_1$) will also lead to an entanglement monotone.

Two natural choices for Δ satisfy requirement (13) and both of them satisfy it with respect to arbitrary operations T (not just LOCC operations): first the trace norm distance $\Delta_1(\rho,\sigma) = \|\rho - \sigma\|_1$ and the relative entropy $\Delta_S(\rho,\sigma) = S(\rho,\sigma)$, leading to entanglement monotones that we denote by E_1 and E_S, respectively. In both the cases, the actual computation of the distance for $\rho,\sigma \in \mathcal{W}$ is greatly simplified by the observation that we may consider both ρ and σ as states (positive normalized linear functionals) on the algebra generated by the permutation operators, and that both the trace norm and the relative entropy are naturally defined for such functionals [10]. Moreover, because the twirl (4) is a conditional expectation, the relative entropy of states in $\mathcal{W}$ is independent of the algebra over which it is computed (cf. Theorem 1.13, [10]). Now the six-dimensional algebra generated by the permutations is independent of the dimension d so that if we parameterize ρ and σ by the expectations of R_k as before, we find that the entanglement monotones E_Δ are independent of dimension. The expression for the relative entropy involves, apart from the abelian summands, the logarithm of a 2×2 matrix, which can also be written explicitly in terms of the parameters r_k for the two states involved. The variational problem (14) can be then solved numerically for arbitrary states in $\mathcal{W}$.

The contour lines over $\mathcal{W}^P$ of the resulting entanglement monotones are plotted in Fig. 6 for E_1 and in Fig. 7 for the relative entropy of tripartite entanglement E_S. Note that the two necessary conditions for $\rho \succ \sigma$ expressed in these diagrams complement each other. In order not to complicate these graphs we have not drawn the simplest sufficient condition for entanglement ordering: from any state ρ, any state lying on a straight line segment ending in $\mathcal{T}$ is less entangled than ρ.

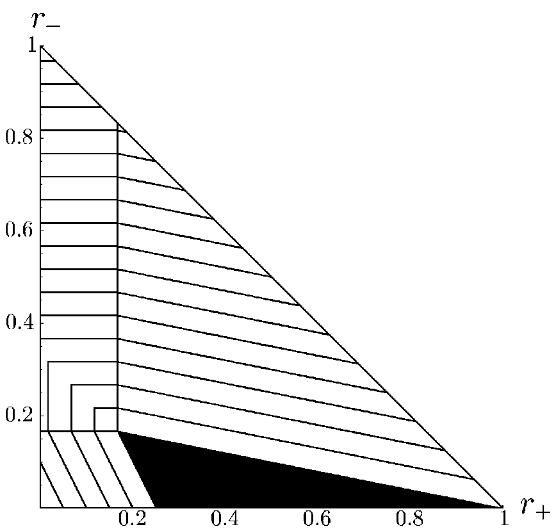

FIG. 6. Contour lines over $\mathcal{W}^P$ for E_1.

As a second section of interest we chose the plane $r_- = 0 = r_1 = r_2$, which is relevant for qubit systems. Qualitatively, it gives the same picture of level lines wrapping around the tripartite set.

V. BISEPARABLE STATES: $\mathcal{B}_1$

In this section we are going to compute the set of biseparable states with respect to the partition $1|23$. The technique is exactly the same as in the triseparable case: we first compute the set $\mathcal{B}_{\text{pure}}$ of states of the form $\mathbf{P}(|\Psi\rangle\langle\Psi|)$ with $|\Psi\rangle\langle\Psi|$ biseparable, i.e., $\Psi = \psi_1 \otimes \psi_{2,3}$. In the second step we get $\mathcal{B}_1$ as the convex hull of $\mathcal{B}_{\text{pure}}$.

We are free to apply to our vector Ψ a $U\otimes U\otimes U$ rotation without changing the projection. In this way we may choose $\psi_1 = |1\rangle$. Now the rotated state Ψ' is of the form $\Psi' = \Sigma_{i,j}\psi_{ij}|1ij\rangle$. The expectations of permutations of such a vector, like

$$\langle\Psi'|V_{(12)}\Psi'\rangle = \sum_{i,j,k,l} \overline{\psi_{ij}}\psi_{kl}\langle 1ij|k1l\rangle = \sum_j |\psi_{1j}|^2$$

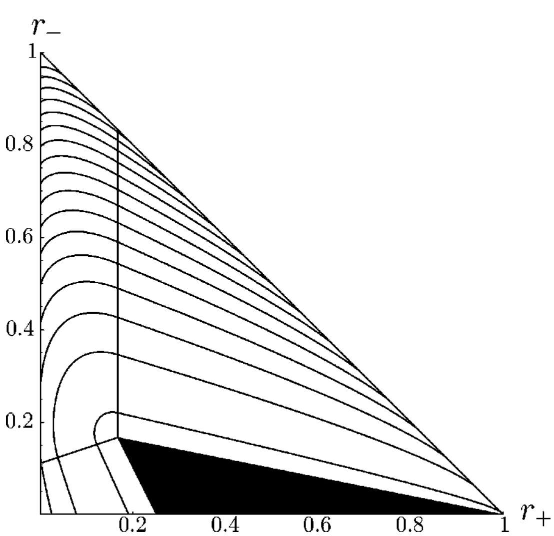

FIG. 7. Contour lines over $\mathcal{W}^P$ for E_S.

then depend linearly on the following real parameters:

$$c_0 = |\psi_{11}|^2, \tag{18a}$$

$$c_1 = \sum_{j>1} |\psi_{1j}|^2, \tag{18b}$$

$$c_2 = \sum_{i>1} |\psi_{i1}|^2, \tag{18c}$$

$$c_3 = \sum_{i,j>1} \overline{\psi_{ij}}\psi_{ji}, \tag{18d}$$

$$c_4 + ic_5 = \sum_{j>1} \overline{\psi_{1j}}\psi_{j1}. \tag{18e}$$

From this we obtain the following r_k:

$$r_+ = \frac{1}{6}(1 + 5c_0 + c_1 + c_2 + c_3 + 4c_4),$$

$$r_- = \frac{1}{6}(1 - c_0 - c_1 - c_2 - c_3),$$

$$r_0 = \frac{2}{3}(1 - c_0 - c_4),$$

$$r_1 = \frac{1}{3}(-c_1 - c_2 + 2c_3 + 4c_4),$$

$$r_2 = \frac{c_1 - c_2}{\sqrt{3}},$$

$$r_3 = \frac{2c_5}{\sqrt{3}}.$$

As in the tripartite case, we need to determine the exact range of the parameters c_i. Let us assume $d>2$ for the moment. By the definitions of c_0, c_1, and c_2 we have

$$c_0, c_1, c_2 \geqslant 0. \tag{19}$$

These parameters fix the weights of the blocks $(i=1, j=1)$, $(i=1, j>1)$, and $(i>1, j=1)$ in the normalization sum $\Sigma_{i,j=1}^d |\psi_{ij}|^2 = 1$. $c_4 + ic_5$ can be read as the scalar product of two $(d-1)$-dimensional vectors $\varphi_1 = (\psi_{12}, \ldots, \psi_{1d})$ and $\varphi_2 = (\psi_{21}, \ldots, \psi_{d1})$ with norm squares $\|\varphi_1\|^2 = c_1$ and $\|\varphi_2\|^2 = c_2$. By the Cauchy-Schwarz inequality we have

$$c_4^2 + c_5^2 = |\langle\varphi_1|\varphi_2\rangle|^2 \leqslant |\varphi_1|^2 |\varphi_2|^2 = c_1 c_2, \tag{20}$$

and any value of $c_4 + ic_5$ consistent with this can actually occur.

We arrange the remaining ψ_{ij} $(i,j>1)$ into a $(d-1)^2$-dimensional vector $\tilde{\Psi} = (\psi_{22}, \ldots, \psi_{2d}, \psi_{32}, \ldots, \psi_{dd})$ with $\|\tilde{\Psi}\|^2 = 1 - c_0 - c_1 - c_2$. On this $(d-1)^2$-dimensional vector space, let U denote the operator swapping ψ_{ij} and ψ_{ji}. Then $c_3 = \langle \tilde{\Psi} | U \tilde{\Psi} \rangle$ is the expectation of an hermitian operator with eigenvalues ± 1. Hence

$$|c_3| \leq \|\tilde{\Psi}\|^2 = 1 - c_0 - c_1 - c_2, \tag{21}$$

and all $c_3 \in \mathbb{R}$ satisfying this inequality can occur.

Together with the obvious modifications in the case $d = 2$, when there is only one index $i > 1$, we get the following lemma:

Lemma 5. A tuple $(c_0, c_1, c_2, c_3, c_4, c_5) \in \mathbb{R}^6$ *arises via* Eqs. (18) *from a unit vector* Ψ *in a* d^2*-dimensional Hilbert space, if and only if* Eqs. (19), (20), *and* (21) *are satisfied and in the case* $d = 2$, *equality holds in* (20) *and* (21).

Let Γ denote the set of tuples $(c_0, c_1, c_2, c_3, c_4, c_5)$ satisfying these constraints. The parameters r_k depend linearly on the c_i although the mapping is not one to one. Nevertheless, any extreme point of $\mathcal{B}_1$ must be the image of an extreme point of the convex hull of Γ.

Hence we can proceed by first determining the extreme points of Γ. Since the positive variables c_0, $|c_3|$ and the sum $(c_1 + c_2)$ are only constrained by inequality (21), every point in Γ is a convex combination of tuples in which only one of these is equal to 1 and the other two vanish. This gives the extreme points (1) $c_0 = 1 \Leftrightarrow \vec{r} = (1,0,0,0,0) \equiv B$, (2) $c_3 = +1 \Leftrightarrow \vec{r} = (\frac{1}{3}, 0, \frac{2}{3}, 0, 0) \equiv D$, (3) $c_3 = -1 \Leftrightarrow \vec{r} = (0, \frac{1}{3}, -\frac{2}{3}, 0, 0) \equiv F$, and furthermore some points with $(c_1 + c_2) = 1$, $c_0 = c_3 = 0$. Eliminating $c_2 = 1 - c_1$, we can write inequality (20) as $c_4^2 + c_5^2 + (c_1 - \frac{1}{2})^2 \leq \frac{1}{4}$. This is a ball with extreme points parameterized by

$$c_0 = 0, \quad c_1 = \frac{1 + \cos(\vartheta)}{2}, \quad c_2 = \frac{1 - \cos(\vartheta)}{2},$$

$$c_3 = 0, \quad c_4 = \frac{\sin(\vartheta)\cos(\varphi)}{2}, \quad c_5 = \frac{\sin(\vartheta)\sin(\varphi)}{2}$$

with $\varphi, \vartheta \in [0, 2\pi]$. By mapping this description of Γ to the r_k-parameterization we come to the following theorem.

Theorem 2. The subset $\mathcal{B}_1 \subset \mathcal{W}$ *of biseparable states with respect to the partition* $1|23$ *has the following extreme points, described here in terms of the expectations* $r_k = \mathrm{tr}(\rho R_k)$, $k = +, -, 1, 2, 3$:

(1) *The sphere given by* $\frac{1}{4}(3r_1 + 1)^2 + 3r_2^2 + 3r_3^2 = 1$ with $r_- = 0$ and $r_+ = (r_1 + 1)/2$ *except for the point* $(\frac{2}{3}, 0, \frac{1}{3}, 0, 0)$, *which is decomposable as* $(\frac{2}{3}, 0, \frac{1}{3}, 0, 0) = \frac{1}{2}(B + D)$.

(2) *The point* $F = (0, \frac{1}{3}, -\frac{2}{3}, 0, 0)$.

(3) The point $D = (\frac{1}{3}, 0, \frac{2}{3}, 0, 0)$.

(4) The point $B = (1,0,0,0,0)$.

A state $\rho \in \mathcal{W}$ *is biseparable with respect to the partition* $1|23$ *if and only if it corresponds to the points F, B or D or the following inequalities are satisfied*:

$$\text{(a)} \quad 0 \leq r_- < \frac{1}{3},$$

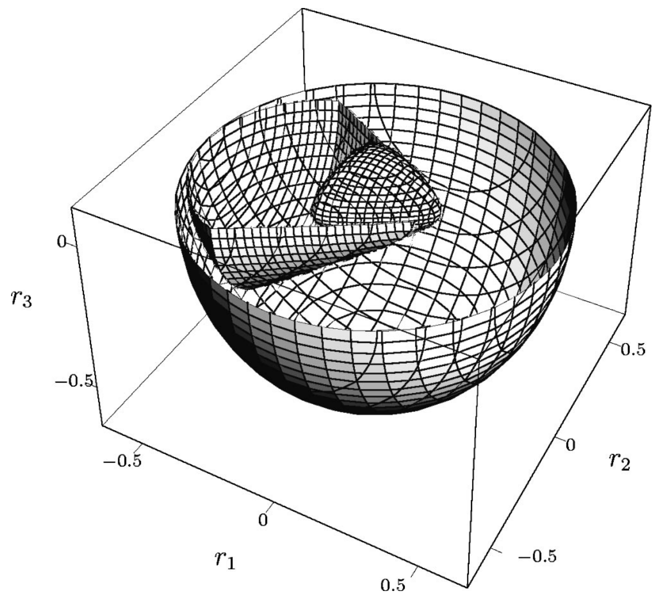

FIG. 8. Plot of the set $\mathcal{B}_1$ as for $r_+ = 0.27$ and $r_- = 0.1$ embedded in the respective Bloch sphere together with $\mathcal{T}$.

$$\text{(b)} \quad -1 < \frac{1 + r_1 - r_- - 2r_+}{1 - 3r_-} < 1,$$

$$\text{(c)} \quad \text{if} \quad -1 < \frac{1 + r_1 - r_- - 2r_+}{1 - 3r_-} \leq 0 \quad \text{then}$$

$$3r_2^2 + 3r_3^2 + (1 + 2r_1 + r_- - r_+)^2 \leq (2 + r_1 - 4r_- - 2r_+)^2$$

$$\text{(d)} \quad \text{if} \quad 0 \leq \frac{1 + r_1 - r_- - 2r_+}{1 - 3r_-} < 1 \quad \text{then}$$

$$3r_2^2 + 3r_3^2 + (1 - 3r_- - 3r_+)^2 \leq (r_1 + 2r_- - 2r_+)^2.$$

We omit here again the computation of these inequalities from the known extreme points. They can be obtained by projecting from the three points F, B, and D onto the sphere of extremal points.

The projection of the set $\mathcal{B}_1$ onto $\mathcal{W}^P$ comes to be equal to the projection of the set of pure $\mathcal{B}_1$-states and was already shown in Fig. 2 together with the section $\mathcal{B}_1 \cap \mathcal{W}^P$. To compare $\mathcal{B}_1$ with $\mathcal{T}$, we plot again the section with $r_+ = 0.27$ and $r_- = 0.1$ (Fig. 8).

To make the inclusion $\mathcal{T} \subseteq (\mathcal{B}_1 \cap \mathcal{B}_2 \cap \mathcal{B}_3)$ mentioned in the introduction more evident we can now compute the sets $\mathcal{B}_2$ and $\mathcal{B}_3$ to build their intersection with $\mathcal{B}_1$. Due to the permutation symmetry of the three subsystems we can rotate $\mathcal{B}_1$ by $\pm 2\pi/3$ in the r_1-r_2-plane instead. This leads to Fig. 9.

VI. POSITIVE PARTIAL TRANSPOSES: $\mathcal{P}_1$

One of the interesting aspects in the theory of bipartite entanglement to emerge in recent years is the consideration of the partial transpose of the density matrix and, in particular, the positivity of the partial transpose. First, this positivity served as a necessary condition for separability, which is even sufficient in $2 \otimes 2$ and $2 \otimes 3$ dimensions (the Peres cri-

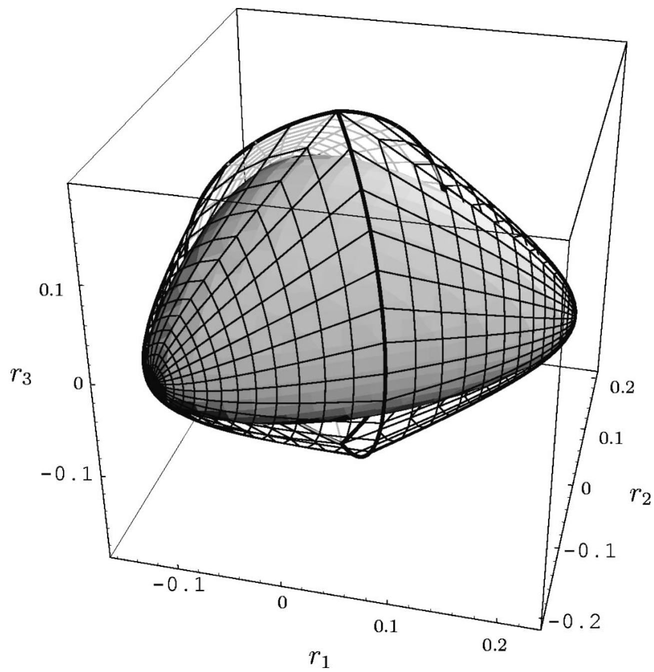

FIG. 9. The intersection $\mathcal{B}_1 \cap \mathcal{B}_2 \cap \mathcal{B}_3$ is shown as a mesh on a transparent surface allowing the set $\mathcal{T}$ to be seen. This plot is again computed for the section $r_+ = 0.27$ and $r_- = 0.1$. The thick lines indicate the intersection of two of the biseparable sets.

terion [5]). Moreover, it is a necessary condition for undistillability, and here it comes much closer to sufficiency even in general situations. Both aspects play a role in the analysis of tripartite states. We will therefore describe in this section the subset $\mathcal{P}_1 \subset \mathcal{W}$ of states with positive 1-transpose.

Since the dimensions for this bipartite system are $d \otimes d^2$, positive partial transpose does not automatically imply biseparability, i.e., the inclusion $\mathcal{B}_1 \subset \mathcal{P}_1$ may be strict. However, since we are considering a special class of states it is also possible that in this class equality holds. This does happen, for example, for the bipartite Werner states [11]. In the tripartite case we will see that $\mathcal{B}_1 = \mathcal{P}_1$ for $d=2$, but not for higher dimensions, although the two sets come to be remarkably close (see Fig. 11). However, the exact description of $\mathcal{P}_1$ is also important for distillation questions.

The partial transpose $A \mapsto A^{T_1}$ of operators on $\mathcal{H}_1 \otimes \mathcal{H}_2$ was defined in Eq. (2). In a tripartite system we take this operation to refer to the first of the three tensor factors and write $\rho \in \mathcal{P}_1$ if $\rho^{T_1} \geqslant 0$.

A. The algebra of partial transposes

When ρ is a linear combination of permutation operators as in Lemma 1, the partial transpose

$$\rho^{T_1} = \sum_\pi \mu_\pi V_\pi^{T_1}$$

is likewise a linear combination of the six operators $V_\pi^{T_1}$, and we have to decide for which coefficients μ_π such an operator is positive. Since partial transposition is *not* a homomorphism, it would appear that the linear combinations of the $V_\pi^{T_1}$ can be a fairly arbitrary space of operators, and deciding positivity could be quite difficult. However, it turns out that these linear combinations do form an algebra, so after the introduction of the right basis deciding positivity is just as easy as determining the state space in Lemma 2.

The abstract reason for this ''happy coincidence'' is that the operators $V_\pi^{T_1}$ span the set of fixed points of an averaging operation in much the same way as the permutations span the set of fixed points of $\mathbf{P}$. The corresponding averaging operator is

$$\tilde{\mathbf{P}}\rho = \int dU (\bar{U} \otimes U \otimes U) \rho (\bar{U} \otimes U \otimes U)^*. \tag{22}$$

Its range consists of all operators commuting with all unitaries of the form $\bar{U} \otimes U \otimes U$, hence is an algebra. The following lemma describes the relation between $\tilde{\mathbf{P}}$ and $\mathbf{P}$.

Lemma 6: *Let A be any Hermitian operator, then*

(1) $\mathbf{P}A = A \Leftrightarrow \tilde{\mathbf{P}}A^{T_1} = A^{T_1}$,

(2) $(\tilde{\mathbf{P}}A)^{T_1} = \mathbf{P}(A^{T_1})$.

Proof. For any Hermitian operator A one has

$$\tilde{\mathbf{P}}A = A \Leftrightarrow [\bar{U} \otimes U \otimes U, A]_- = \mathbf{0}$$
$$\Leftrightarrow [U \otimes U \otimes U, A^{T_1}]_- = \mathbf{0}$$
$$\Leftrightarrow \mathbf{P}A^{T_1} = A^{T_1}.$$

Furthermore, we can compute directly

$$\mathbf{P}A^{T_1} = \int dU (U \otimes U \otimes U) A^{T_1} (U \otimes U \otimes U)^*$$
$$= \int dU [(\bar{U} \otimes U \otimes U) A (\bar{U} \otimes U \otimes U)^*]^{T_1}$$
$$= (\tilde{\mathbf{P}}A)^{T_1}.$$

■

For deciding positivity of partial transposes we need a concrete form of the algebra spanned by the partial transposes of the permutation operators. For example, we get

$$V_{(12)}^{T_1} = \sum_{ijk} (|ijk\rangle\langle jik|)^{T_1}$$
$$= \sum_{ijk} |jjk\rangle\langle iik|$$
$$= (|\Phi\rangle\langle\Phi|) \otimes \mathbb{1},$$

where $\Phi = \Sigma_i |ii\rangle$ is a maximally entangled vector of norm d. The partial transposes of the other permutations are computed similarly. We can express all of them in terms of the first two:

$$X = V_{(12)}^{T_1} \quad \text{and} \quad V = V_{(23)}^{T_1} = V_{(23)} \tag{23}$$

as

$$\mathbb{1}^{T_1} = \mathbb{1}, \quad V_{(13)}^{T_1} = VXV, \quad V_{(123)}^{T_1} = XV, \quad V_{(321)}^{T_1} = VX.$$

Then these operators satisfy the relations $X^*=X$, $V^*=V$ and

$$X^2=dX, \quad V^2=\mathbb{1}, \quad XVX=X. \tag{24}$$

Due to these relations the set of linear combinations of the six operators $\{\mathbb{1},X,VXV,V,XV,VX\}$ is closed under adjoints and products. Positivity of such linear combinations, and hence the positivity of all partial transposes of operators in $\mathcal{W}$ can therefore be decided by studying the abstract algebra generated by two hermitian elements X and V satisfying Eq. (24). As a six-dimensional noncommutative C* algebra it is isomorphic to the algebra generated by the permutations, i.e., a sum of two one-dimensional and a two-dimensional matrix algebra. But of course, the partial transpose operation mapping one into the other is not a homomorphism.

From these considerations it is clear that all we have to do now is to find a basis of the algebra generated by X and V analogous to the basis (5). This sort of computation can be quite painful, so we recommend the use of a symbolic algebra package. The result is

$$S_+=\frac{\mathbb{1}+V}{2}\left(\mathbb{1}-\frac{2X}{d+1}\right)\frac{\mathbb{1}+V}{2}, \tag{25a}$$

$$S_-=\frac{\mathbb{1}-V}{2}\left(\mathbb{1}-\frac{2X}{d-1}\right)\frac{\mathbb{1}-V}{2}, \tag{25b}$$

$$S_0=\frac{1}{d^2-1}[d(X+VXV)-(XV+VX)], \tag{25c}$$

$$S_1=\frac{1}{d^2-1}[d(XV+VX)-(X+VXV)], \tag{25d}$$

$$S_2=\frac{1}{\sqrt{d^2-1}}[X-VXV], \tag{25e}$$

$$S_3=\frac{i}{\sqrt{d^2-1}}(XV-VX). \tag{25f}$$

These operators satisfy exactly the same relations as R_k from Eq. (5) and we will denote the corresponding expectation values by $s_k(\rho):=\mathrm{tr}(\rho S_k)$. The two projections $S_\pm$ correspond to the two one-dimensional representations of the algebra, i.e., to the two realizations of the relations by c numbers, namely, $X=0,V=1$ and $X=0,V=-1$.

B. The $V_{(23)}$-invariant case

The simplest case is the $V_{(23)}$-invariant subset of $\mathcal{W}$ as it is a three-dimensional object. In fact the $V_{(23)}$ invariance implies the conditions $\mathrm{tr}(\rho V_{(23)})=1$, $\mathrm{tr}(\rho V_{(12)})=\mathrm{tr}(\rho V_{(31)})$, and $\mathrm{tr}(\rho V_{(123)})=\mathrm{tr}(\rho V_{(321)})$. Therefore, we have $r_2=r_3=0$. In the same way we obtain for a $V_{(23)}$-invariant state $\rho\in\mathcal{W}^{T_1}$ the conditions $s_2=0$ and $s_3=0$. Positivity of a $V_{(23)}$-invariant state in $\mathcal{W}$ requires now $r_+\geqslant 0$, $r_-\geqslant 0$ and $|r_1|\leqslant r_0=1-r_+-r_-$ [cf. (6)] giving rise to a tetrahedron bounded by the hyperplanes

$$(h_1)r_+=0, \quad (h_2)r_-=0, \quad (h_3)r_1=1-r_+-r_-,$$
$$(h_4)r_1=r_++r_--1$$

and having the extreme points $P_1=(0,0,1)$, $P_2=(0,0,-1)$, $P_3=(0,1,0)$, and $P_4=(1,0,0)$. The same computation can be done on the partially transposed side leading to the tetrahedron confined by the hyperplanes

$$(h_1')s_+=0, \quad (h_2')s_-=0, \quad (h_3')s_1=1-s_+-s_-,$$
$$(h_4')s_1=s_++s_--1.$$

Using Lemma 6 we can express s_k by r_k of the corresponding $\mathcal{W}$ state. Multiplying by positive constants one gets an easier description of these hyperplanes.

$$(h_1')2(1+r_1-r_--2r_+)+d(1+r_1-r_-+r_+)=0,$$
$$(h_2')2(-1+r_1+2r_-+r_+)+d(1-r_1+r_--r_+)=0,$$
$$(h_3')1-r_1-5r_--r_+=0,$$
$$(h_4')1+r_1-r_--5r_+=0.$$

Its four extremal points are now $Q_1=((2+d)/3,0,(1-d)/3)$, $Q_2=(0,(2-d)/3,-(1+d)/3)$, $Q_3=(0,\frac{1}{3},-\frac{2}{3})$, and $Q_4=(\frac{1}{3},0,\frac{2}{3})$. Of course, these points have no reason to correspond to positive states, and indeed only Q_3 and Q_4 lie inside the state space, where Q_1 and Q_4 are outside the state space for all d.

As we are looking for those $V_{(23)}$-invariant $\mathcal{W}$-states that have positive partial transpose, i.e. that lie in $\mathcal{P}_A$, we now have to look at the intersection of these two tetrahedra. The resulting object is again a tetrahedron as one can see in Fig. 10. This is due to the fact that the extremal points P_i and $Q_i(i=1,2,3,4)$ lie on just two straight lines, namely $\overline{P_1Q_4P_4Q_1}$ and $\overline{Q_2P_2Q_3P_3}$. The intersection of the two tetrahedra is hence again a tetrahedron, spanned by the extremal points P_2, P_4, Q_3, and Q_4 (called E, B, F, and D in Secs. II B and V), and is thus dimension independent. But it is easily verified from Theorem 2 that these four points are precisely the extreme points of the $V_{(23)}$-invariant part of $\mathcal{B}_1$. Since $\mathcal{B}_1\subset\mathcal{P}_1$, we have shown the following:

Lemma 7. A $V_{(23)}$-invariant $\mathcal{W}$ state has a positive partial transpose if and only if it is biseparable.

As we will see in the next subsection, the assumption of $V_{(23)}$ invariance is essential, i.e., the conclusion does not hold for general $\mathcal{W}$ states.

In order to see how $V_{(23)}$ invariance helps, we conclude this subsection with a direct proof of the above lemma for $d=2$. If ρ is a $V_{(23)}$-invariant $\mathcal{W}$-state, then we can decompose it into the following sum:

$$\rho=\frac{1}{4}(\mathbb{1}+V_{(23)})\rho(\mathbb{1}+V_{(23)})+\frac{1}{4}(\mathbb{1}-V_{(23)})\rho(\mathbb{1}-V_{(23)})$$

$$=:\rho^{+}+\rho^{-}.$$

It is now clear that ρ has a positive partial transpose if both ρ^{+} and ρ^{-} have a positive partial transpose. ρ^{+} denotes the $V_{(23)}$-symmetric part of ρ and ρ^{-} the antisymmetric part. Thus we know that ρ^{+} is a 2×3-density operator and ρ^{-} a 2×1. For these systems the Peres criterion holds strictly [12], i.e., states have a positive partial transpose if they are separable or, in our case, biseparable over the $1|23$ split. Biseparability of ρ^{+} and ρ^{-} is equivalent to the biseparability of ρ, which proves the lemma. ■

C. The general case

The positivity conditions for arbitrary linear combinations of the operators S_k give the following result.

Lemma 8. Let $\rho\in\mathcal{W}$ *be a density operator with expectations* $r_k=\mathrm{tr}(\rho R_k)$, $k=+,-,1,2,3$. *Then the partial transpose of* ρ *with respect to the first tensor factor is positive, i.e.,* $\rho\in\mathcal{P}_1$ *if and only if*

$$0\leqslant r_{-}, \tag{26a}$$

$$0\leqslant r_1-r_{+}-r_{-}+1, \tag{26b}$$

$$0\leqslant 1-r_1-5r_{-}-r_{+}, \tag{26c}$$

$$0\leqslant -1-r_1+r_{-}+5r_{+}, \tag{26d}$$

$$r_2^2+r_3^2\leqslant R_1, \tag{26e}$$

$$r_2^2+r_3^2\leqslant R_2, \tag{26f}$$

where

$$R_1:=(1-r_1-5r_{-}-r_{+})(-1-r_1+r_{-}+5r_{+})/3,$$

$$R_2:=(1-r_1-r_{-}-r_{+})(1+r_1-r_{-}-r_{+}).$$

Proof. Recall that averaging with respect to $V_{(23)}$ projects $\mathcal{P}_1$ to the section of $\mathcal{P}_1$ with $r_2=r_3$. Therefore, the inequalities describing the tetrahedron discussed in the last subsection are optimal. These are the first four inequalities. We therefore only have to describe the admissible set of (r_2,r_3) for given (r_+,r_-,r_1). There are two conditions to consider, one from the positivity of ρ and the other from the positivity of ρ^{T_1}. As shown in the first subsection, both these requirements have a very similar form, namely the positivity of an element in an abstract algebra with two one-dimensional summands and one summand isomorphic to the 2×2-matrices. Now, in both the cases, (r_+,r_-,r_1) are readily seen to fix the weights of the one-dimensional parts as well as the trace and the expectation of the first Pauli matrix for the 2×2-part. This leaves a condition of the form $r_2^2+r_3^2\leqslant R$ in both cases. The two conditions are given in the Lemma, where $R_2=(1-r_+-r_-)^2-r_1^2$ expresses the requirement $\rho\geqslant 0$. The condition (26e) is obtained from $\rho^{T_1}\geqslant 0$ by expressing ρ^{T_1} in the basis S_k and applying the same criterion to the expectations s_k. ■

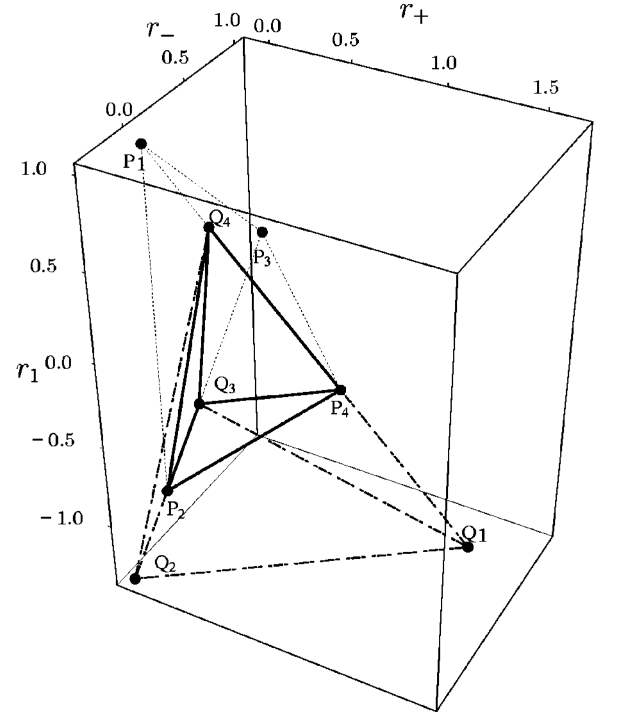

FIG. 10. The two positivity tetrahedra bounded by h_i (dotted), h_i' (dashed), and the intersection tetrahedron (solid lines) for $d=3$.

According to this lemma the set $\mathcal{P}_1$ can be visualized as follows: first, one has to fix a point (r_+,r_-) in the permutation-invariant triangle (Fig. 2). The possible choices of (r_1,r_2,r_3) can then be seen from Fig. 8. Apart from the heart-shaped tripartite set in the center this figure contains three quadratic surfaces: the Bloch sphere and the two surfaces bounding $\mathcal{B}_1$. Comparing condition (d) of Theorem 2 and the expression for R_1 given in the above lemma, we find that both constraints are given by the same hyperboloid, the one wrapped around the tripartite set in Fig. 8. Hence in this figure we can readily find $\mathcal{P}_1$ by extending this hyperboloid all the way to the Bloch sphere and taking the intersection. This is shown in Fig. 11, in the section $r_3=0$.

Figure 11 shows the generic situation with $r_-\neq 0$. When $r_-=0$, in particular, for systems of three qubits, the boundary ellipsoid of $\mathcal{B}_1$, described by condition (c) of Theorem 2, coalesces with the Bloch sphere. This leads to another instance where the Peres-Horodecki criterion for separability holds.

Corollary 1. The intersections of $\mathcal{B}_1$ *and* $\mathcal{P}_1$ *with the plane* $r_-=0$ *coincide. In particular, for* 3*-qubit* $\mathcal{W}$ *states, biseparability is equivalent to the positivity of the partial transpose*.

We conclude this section by the explicit determination of the extreme points of $\mathcal{P}_1$. From Fig. 11 it might appear that all points on the quadratic surfaces bounding $\mathcal{P}_1$ might be extremal. But this is misleading because we also have to take into account the possibility of decompositions with different values of (r_+,r_-). In fact, for the inequalities arising from

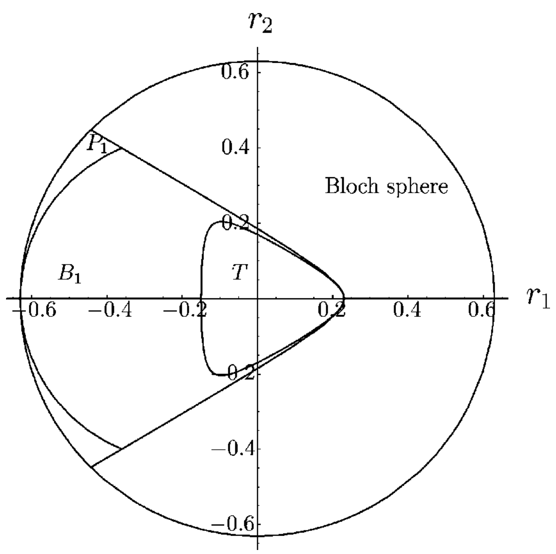

FIG. 11. Plot of the Bloch sphere, $\mathcal{T}$, $\mathcal{B}_1$, and $\mathcal{P}_1$ for $r_+ = 0.27$, $r_- = 0.1$, and $r_3 = 0$.

$\rho \geqslant 0$, it is evident that generically such decompositions are possible: given any $(r_+, r_-, r_1, r_2, r_3)$, which lies on the Bloch sphere in Fig. 11, we can just change the weights of the three blocks in the block decomposition of ρ according to $(\lambda_+ r_+, \lambda_- r_-, \lambda_0 r_1, \lambda_0 r_2, \lambda_0 r_3)$, as long as λ_α's are positive and the normalization $\lambda_+ r_+ + \lambda_- r_- + \lambda_0(1 - r_+ - r_-) = 1$ is respected. This leaves a two-dimensional affine manifold through $(r_+, r_-, r_1, r_2, r_3)$. Hence, unless other conditions constraining $\mathcal{P}_1$ prevent the indicated decompositions, no such point will be extremal. Of course, the second constraint (26e) has the same structure because the algebra of partial transposes is isomorphic to the algebra generated by the states. Hence in Fig. 11 only the points in the intersection of the hyperboloid and the Bloch sphere remain as candidates for extreme points. This is analogous to the extreme points of $\mathcal{B}_1$, which also consist of the intersection of two quadratic surfaces in Fig. 11. For $\mathcal{P}_1$ we get the following.

Theorem 3. The subset $\mathcal{P}_1 \subset \mathcal{W}$ of $\mathcal{W}$-states with positive 1-transpose has the following extreme points, described here in terms of the expectations $r_k = \mathrm{tr}(\rho R_k)$, $k = +, -, 1, 2, 3$.

(1) *The points P_2, Q_3, P_4, and Q_4, which also span the $V_{(23)}$-invariant part of $\mathcal{P}_1$.*

(2) *The remaining extreme points of $\mathcal{B}_1$, which form a sphere in the $r_- = 0$ plane* (cf. *Theorem 2*).

(3) *The points for which $(r_+, r_-, r_1, 0, 0)$ lie in the interior of the $V_{(23)}$-invariant tetrahedron and for which inequalities* (26e) *and* (26f) *are both satisfied with equality*.

Proof. Let us first discuss the periphery of the tetrahedron. Every face of the tetrahedron corresponds to a face of $\mathcal{P}_1$, namely, the face of points projecting to it upon $V_{(23)}$-averaging. In Lemma 8 this corresponds to the subsets for which one of the linear inequalities (26a)–(26d) is an equality. We will show first that each of these faces is actually contained in $\mathcal{B}_1$. Indeed, when (26b), (26c), or (26d) are equalities, one of the factors in R_1 or R_2 vanishes, forcing

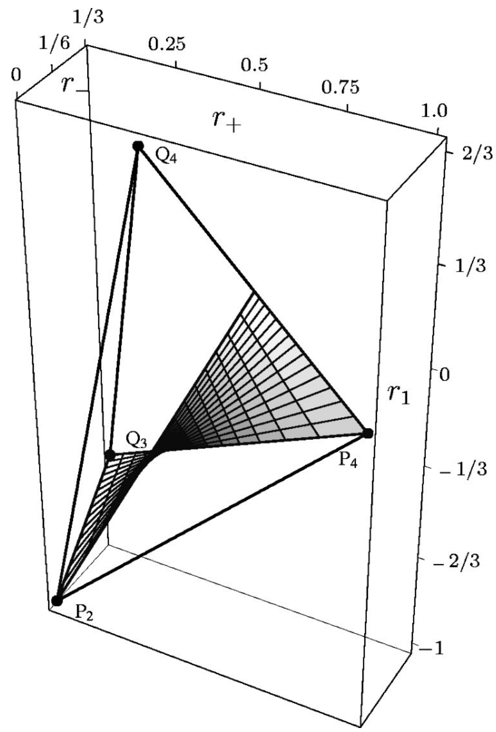

FIG. 12. Section of the intersecting tetrahedron with the separating one-leaf hyperboloid.

$r_2 = r_3 = 0$ and reducing our claim to Lemma 7. When (26a) is an equality, i.e., $r_- = 0$, the claim is contained in Corollary 1.

Now a point of $\mathcal{P}_1$ contained in one of these faces can only have decompositions in the same face, hence in $\mathcal{B}_1$, for such a point, extremality in $\mathcal{P}_1$ and extremality in $\mathcal{B}_1$ are equivalent.

It remains to show item 3 of the theorem, i.e., to characterize the extreme points of $\mathcal{P}_1$ whose $V_{(23)}$ averages fall in the interior of the tetrahedron. From the arguments preceding the theorem, it is clear that the points for which only one of the inequalities (26e) and (26f) is an equality cannot be extremal since the surfaces defined by these inequalities contain straight lines. Therefore, the condition stated in the theorem is necessary for a point to be extremal. It remains to show that none of the points with $R_1 = R_2$ can be decomposed in a proper convex combination.

Let us denote by M_1 (M_2) the set of points in the interior of the tetrahedron such that $R_1 \leqslant R_2$ ($R_2 \leqslant R_1$). The intersection $M_* = M_1 \cap M_2$ of these sets is described by the condition $R_1 = R_2$, or explicitly

$$r_1^2 + 3r_- + r_1 r_- - 2r_-^2 + 3r_+ - r_1 r_+ - 8r_- r_+ - 2r_+^2 = 1. \tag{27}$$

This is a one-sheet hyperboloid generated by two sets of straight lines shown in Fig. 12. Consider a line segment

$$u \mapsto (\hat{r}_+, \hat{r}_-, \hat{r}_1) + u(t_+, t_-, t_1) \tag{28}$$

through one of the points $\hat{p}=(\hat{r}_+,\hat{r}_-,\hat{r}_1)\in M_*$ of the hyperboloid. Also consider the radius functions $\sqrt{R_i}$ evaluated as a function of the parameter u. If such a function is affine (has vanishing second derivative) we can set $(r_1(u),r_2(u))=(\cos\alpha,\sin\alpha)\sqrt{R_i}$ with arbitrary α to get a straight line in the corresponding hypersurface in five dimensions. We then call (t_+,t_-,t_1) an *affine direction* for R_i. Along other directions R_i is strictly concave, so no decomposition along the segment (28) is possible. For both radius functions, the set of affine directions is a two-dimensional plane and thus best described by its normal vector. That is, $\vec{t}=(t_+,t_-,t_1)$ is an affine direction for R_i if $\vec{t}\cdot\vec{A}_i=0$, where

$$\vec{A}_1=\begin{pmatrix} 2-3\hat{r}_1-12\hat{r}_- \\ -2-3\hat{r}_1+12\hat{r}_+ \\ -1+3\hat{r}_-+3\hat{r}_+ \end{pmatrix}, \quad \vec{A}_2=\begin{pmatrix} -\hat{r}_1 \\ -\hat{r}_1 \\ -1+\hat{r}_-+\hat{r}_+ \end{pmatrix}. \tag{29}$$

Assuming that a convex decomposition along Eq. (28) is possible, we thus arrive at a threefold case distinction.

(1) The line segment lies entirely in M_1. Then it must be tangent to the hyperboloid M_* and also an affine direction for R_1. The vector $\vec{t}$ is uniquely determined up to a factor by these conditions. However, that does not mean that the corresponding line segment lies in M_1, and in fact, one can show that it *never* does. Hence this case is ruled out.

(2) The line segment lies entirely in M_2. This is ruled out analogously.

(3) The line segment crosses from M_1 into M_2. Then $\vec{t}$ must be affine for both radius functions. Again, this determines $\vec{t}$ to within a factor. But for a proper decomposition we must also have that the slopes of $\sqrt{R_1}$ and $\sqrt{R_2}$ match at $u=0$. One can show that this never happens inside the tetrahedron we discuss, so this case is also ruled out.

We conclude that no point on M_* allows a convex decomposition inside $\mathcal{P}_1$, and the theorem is proved.

ACKNOWLEDGMENTS

We would like to thank M. Horodecki for discussions. Funding by the European Union project EQUIP (Contract No. IST-1999-11053) and financial support from the DFG (Bonn) are gratefully acknowledged.

APPENDIX ANALYSIS OF $\tilde{\mathbf{P}}$

In this appendix we give a characterization of the separability classes ($\tilde{\mathcal{T}}$, $\tilde{\mathcal{B}}_1$, and $\tilde{\mathcal{P}}_1$) of $\tilde{\mathbf{P}}$ showing that they can be deduced from those of $\mathbf{P}$ without any computation.

The intimate relation between the two twirls emerged already in Lemma 6 where we stated the existence of an isomorphism between the two algebras spanning the eigenspaces of $\mathbf{P}$ and $\tilde{\mathbf{P}}$. This isomorphism establishes an affine mapping ι between the two eigenspaces that we used to compute $\mathcal{P}_1$. Due to the inclusion $\mathcal{T}\subsetneq\mathcal{B}_1\subsetneq\mathcal{P}_1$ it is clear that the same mapping transports the sets $\mathcal{T}$ and $\mathcal{B}_1$ to their counterparts $\tilde{\mathcal{T}}$ and $\tilde{\mathcal{B}}_1$. The mapping ι can be computed by fixing the ordering $\{\mathbb{1},X,V,VXV,XV,VX\}$ for the second algebra and concatenating the transformations (5) and (25) getting

$$\vec{s}=\iota\vec{r}$$

with

$$\iota=\begin{pmatrix} \frac{d-1}{d+1} & 0 & \frac{d+2}{2d+2} & \frac{d+2}{2d+2} & 0 & 0 \\ 0 & \frac{d+1}{d-1} & \frac{d-2}{2d-2} & \frac{2-d}{2d-2} & 0 & 0 \\ \frac{2}{d+1} & -\frac{2}{d-1} & \frac{1}{d^2-1} & -\frac{d}{d^2-1} & 0 & 0 \\ \frac{2}{d+1} & \frac{2}{d-1} & -\frac{d}{d^2-1} & \frac{1}{d^2-1} & 0 & 0 \\ 0 & 0 & 0 & 0 & \frac{\sqrt{3}}{\sqrt{d^2-1}} & 0 \\ 0 & 0 & 0 & 0 & 0 & \frac{\sqrt{3}}{\sqrt{d^2-1}} \end{pmatrix}.$$

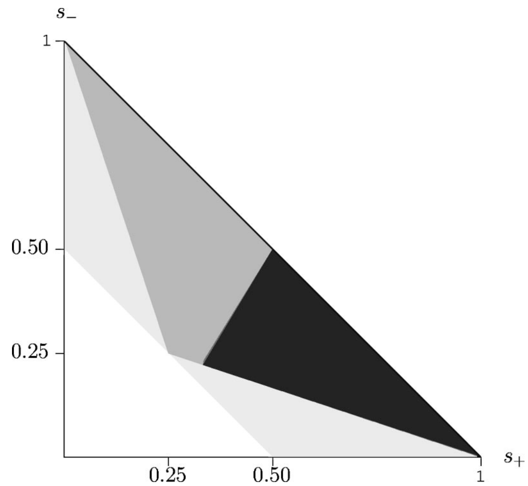

FIG. 13. Sections and projections of $\tilde{\mathcal{T}}$ and $\tilde{\mathcal{B}}_1$ with/onto the s_+-s_- plane for $d=3$. Black, section with $\tilde{\mathcal{T}}$; dark gray, projection of $\tilde{\mathcal{T}}$; and light gray, section with $\tilde{\mathcal{B}}_1$.

With this mapping we can compute directly the $\tilde{\mathbf{P}}$ projection of the states A to G:

$$A:|123\rangle\rightarrow(1/2,1/2,0,0,0)$$

$$B:|111\rangle\rightarrow\left(\frac{d-1}{d+1},0,\frac{2}{d+1},0,0\right)$$

$$C:(|111\rangle-\sqrt{3}|112\rangle+\sqrt{3}|121\rangle-3|122\rangle)/4$$

$$\rightarrow\left(\frac{4+5d}{8+8d},\frac{3d-6}{8d-8},\frac{d+2}{4-4d^2},0,0\right)$$

$$D:|122\rangle\rightarrow(1,0,0,0,0)$$

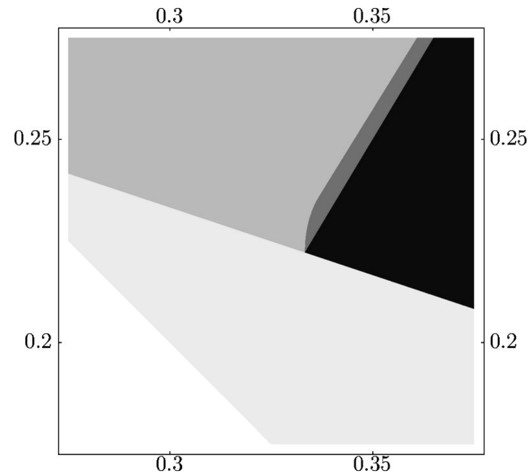

FIG. 14. Zoomed region of Fig. 11.

$$E:(|112\rangle-|121\rangle)/\sqrt{2}\rightarrow\left(0,\frac{d-2}{d-1},\frac{1}{1-d},0,0\right)$$

$$F:(|123\rangle-|132\rangle)/\sqrt{2}\rightarrow(0,1,0,0,0)$$

$$G:(|112\rangle-|121\rangle-\sqrt{3}|122\rangle)/\sqrt{5}\rightarrow\left(\frac{3}{5},\frac{2d-4}{5d-5},\frac{2}{5-5d},0,0\right)$$

Applying the transformation to the extremal points and inequalities of Theorems 1, 2, and 3 yields then a characterization of $\tilde{\mathcal{T}}$, $\tilde{\mathcal{B}}_1$, and $\tilde{\mathcal{P}}_1$.

We omit here the results of these transformations and give Fig. 13, which corresponds to Fig. 2.

In contrast to what can be seen in Fig. 2, the projection of $\tilde{\mathcal{T}}$ onto the s_+-s_- plane differs from its section with it as one can see in Fig. 14.

[1] R. F. Werner, Phys. Rev. A **40**, 4277 (1989).
[2] S. Popescu, Phys. Rev. Lett. **72**, 797 (1994).
[3] C. H. Bennett, D. P. DiVincenzo, J. A. Smolin, and W. K. Wootters, Phys. Rev. A **54**, 3824 (1996).
[4] W. Dür, J. I. Cirac, and R. Tarrach, Phys. Rev. Lett. **83**, 3562 (1999).
[5] A. Peres, Phys. Rev. Lett. **77**, 1413 (1996).
[6] C. H. Bennett *et al.*, Phys. Rev. Lett. **82**, 5385 (1999).
[7] H. Weyl, *The Classical Groups* (Princeton University, Princeton, NJ, 1946).
[8] A. Elby and J. Bub, Phys. Rev. A **49**, 4213 (1994).
[9] M. A. Nielsen, Phys. Rev. Lett. **83**, 436 (1999).
[10] M. Ohya and D. Petz, *Quantum Entropy and Its Use* (Springer, New York, 1993).
[11] M. Horodecki and P. Horodecki, Phys. Rev. A **59**, 4206 (1999).
[12] M. Horodecki, P. Horodecki, and R. Horodecki, Phys. Lett. A **223**, 1 (1996).